Calculation of x-ray single scattering in diagnostic radiology

To cite this article: L R M Morin and A Berroir 1983 *Phys. Med. Biol.* **28** 789

Phys. Med. Biol., 1983, Vol. 28, No. 7, 789–797. Printed in Great Britain

Calculation of x-ray single scattering in diagnostic radiology

L R M Morin† and A Berroir‡

† 15 Avenue Bosquet, 75007 Paris, France
‡ Laboratoire de Météorologie Dynamique du CNRS, Ecole Normale Supérieure, 75231 Paris, France

Received 15 September 1982, in final form 20 December 1982

Abstract. Single-scattered energy has been calculated for a water phantom, in a geometrical arrangement that approaches that of the dynamic spatial reconstructor. Recent data on the Rayleigh differential cross-sections of liquid water have been used. The ratio for single-scattered to transmitted radiation is found to be dependent upon incident energy: in the range 20 to 80 keV, it varies from 0.32 to 0.16. The contribution of the Rayleigh effect to single scattering is of the order of 90% at 20 keV and 50% at 80 keV.

1. Introduction

There are at present three types of x-ray diagnostic apparatus: (i) the apparatus of conventional x-ray radiology; (ii) the CT scanners (a recent review has been published by Schultz and Felix (1980)); and (iii) the dynamic spatial reconstructor (DSR), which is being developed at the Mayo Clinic, Minnesota (Kinsey and Orvis 1981).

In each of these systems, the presence of scattering reduces the quality of imaging. In addition to the classical collimated grids, various antiscatter devices have been developed, especially by Moore *et al* (1976), Rudin and Bednarek (1980), Cacak (1981). Joseph and Spital (1981) have developed an algorithm to correct some of the scattering artefacts. Stonestrom and Macovski (1976) have proposed to measure the scattered energy by an additional detector array located just outside the limits of the primary beam.

Experimental studies of x-ray scattering in radiodiagnosis have been carried out by Stargardt and Angerstein (1975), Dick *et al* (1978), Levine and Hale (1980) and Burgess and Pate (1981). Monte Carlo calculations have been carried out by Reiss and Steinle (1973) and by Kalender (1981). These calculations assume that the scattering properties of water can be derived from the individual atomic scattering properties of hydrogen and oxygen.

The aim of this paper is to calculate the energy which is single-scattered in medical x-ray diagnosis, taking into account the specific coherent scattering properties of liquid water.

2. Geometry of the calculations

2.1. Pencil beam

The irradiated water phantom is considered to have rotational symmetry around the axis (Oz) of the incident pencil beam. The detectors are assumed to be placed on a

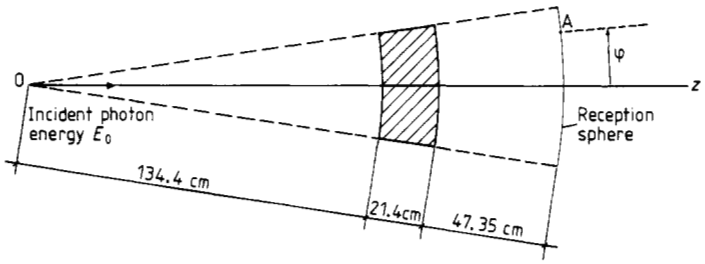

Figure 1. Geometry of the calculations: pencil beam. The figure has rotational symmetry around the $0z$ axis.

sphere called the 'reception sphere' (figure 1). The position of a point A located on the reception sphere is defined by the angle φ.

2.2. Conical beam

The incident conical beam is assumed to be monoenergetic. The geometrical arrangement shown in figure 2 has been chosen as it approaches that of the DSR (Kinsey and Orvis 1981). The device is assumed to have rotational symmetry around the Oz axis. This assumption enables us to calculate the scattered energy in this case from the results of the pencil beam calculations, while it introduces only slight differences from the arrangement effectively used in the DSR.

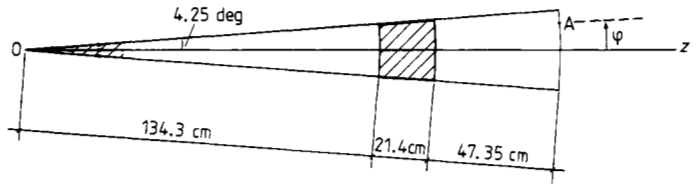

Figure 2. Geometry of the calculations: conical beam. The figure has rotational symmetry around the $0z$ axis. Half angle of the cone = 4.25°.

3. Data on the interaction effects

In the energy range 20–80 keV, three interaction processes between photons and matter must be taken into account: the photoelectric effect, the Compton effect, and the Rayleigh effect. The incident beam is assumed to be unpolarised. This legitimises: (i) the use of the Klein–Nishina differential cross-section for unpolarised radiation (see section 3.2); and (ii) the use of the Thomson formula weighted by the square of the form factor (see section 3.3).

3.1. Photoelectric effect

For light elements and photon energies greater than 20 keV, the photoeffect does not, in practice, contribute to the scattering: almost all the energy of the interacting photon is absorbed by the recoil electron.

Because of the lack of data on the molecular photoeffect cross-section σ_w^{ph} of water, it was assumed that σ_w^{ph} could be calculated according to the formula

$$\sigma_w^{ph} = \sigma_O^{ph} + 2\sigma_H^{ph} \tag{1}$$

where σ_O^{ph} and σ_H^{ph} are the atomic photoeffect cross-sections of oxygen and hydrogen, calculated from theoretical results of Scofield (1973).

3.2. Compton effect

Because of the lack of data on the molecular Compton cross-section σ_w^C of water, it was assumed that σ_w^C could be calculated according to the formula:

$$\sigma_w^C = \sigma_O^C + 2\sigma_H^C \tag{2}$$

where σ_O^C and σ_H^C are the theoretical atomic Compton cross-sections of oxygen and hydrogen, given by Hubbell *et al* (1975).

The differential Compton cross-section of water was calculated from the Klein–Nishina differential cross-section for unpolarised radiation, weighted by the molecular incoherent scattering function S_w of water. Due to the lack of data on this function, S_w was calculated according to the formula

$$S_w = S_O + 2S_H \tag{3}$$

where S_O and S_H are the theoretical atomic incoherent scattering functions of oxygen and hydrogen, given by Hubbell *et al* (1975).

3.3. Rayleigh effect

In the Rayleigh effect, the energies of the incident and scattered photons are practically the same; the energy change is equal to the small amount of energy taken up by the scattering atom or molecule and is negligible (Moon 1950). Thus the Rayleigh effect is a coherent scattering process which gives rise to interference effects. These interference effects are mostly important in the forward direction, where the path length differences are small (James 1962).

As the incident beam has been assumed to be unpolarised, the Rayleigh differential cross-section of water can be obtained by weighting the Thomson formula by the square of the water form factor F_w. Three different form factors F_w can be used: $F_{w,at}$, $F_{w,mol}$, $F_{w,liq}$ (Morin, to be published).

(i) $F_{w,at}$ is the form factor of water in the independent atomic scattering approximation, calculated according to the formula:

$$F_{w,at}^2 = F_O^2 + 2F_H^2 \tag{4}$$

where F_O and F_H are the atomic form factors of oxygen and hydrogen. In this approximation, each atom of the water molecule is supposed to radiate by itself, independently from the others. Inter-atomic interference effects are not taken into account.

(ii) $F_{w,mol}$ is the form factor of a free water molecule: it has been calculated by Blum (1971). In this case, only the interference effects which occur within the water molecule are taken into account.

(iii) $F_{w,liq}$ is the molecular form factor of liquid water: it can be derived from the experimental data of Narten and Levy (1971). In this case, all the interference effects are taken into account, including the inter-molecular interference effects which occur in liquid water.

Figure 3 shows $F_{w,at}$, $F_{w,mol}$ and $F_{w,liq}$ plotted against $x = \sin(\theta/2)/\lambda$, θ being the scattering angle and λ the wavelength of the incident radiation. Differences between

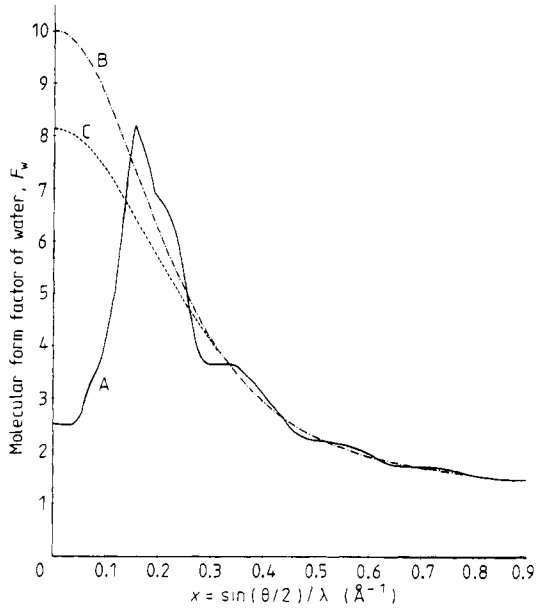

Figure 3. Molecular form factors of water. Curve A, $F_{w,liq}$, for liquid water, derived from the experimental results of Narten and Levy (1971). Curve B, $F_{w,mol}$ for free water molecule, theoretical results of Blum (1971). Curve C, $F_{w,at}$, independent atomic scattering approximation, calculated from the theoretical atomic form factors of oxygen and hydrogen, given by Hubbell and Overbo (1979).

$F_{w,mol}(x)$ and $F_{w,liq}(x)$ are due to the inter-molecular interference effects which take place in liquid water. The difference between $F_{w,mol}(0)$ and $F_{w,liq}(0)$ arises from the fact that the coherent scattering intensity by fluids at zero angle is related to density and to isothermal compressibility. The ratio $F_{w,liq}(0)/F_{w,mol}(0)$ reflects the fluctuation of the number of molecules in a given volume of liquid water (Guinier 1964). It is given by the formula, (derived from Guinier 1964)

$$F_{w,liq}(0)/F_{w,mol}(0) = (k\beta T/v)^{1/2}$$

where k is Boltzmann's constant, T the temperature in degrees Kelvin, v the average volume offered to each molecule of liquid water, and β the isothermal compressibility of liquid water.

For the free water molecule, the form factor to be used is $F_{w,mol}$. For the water molecule in the gas, the form factor $F_{w,mol}$ can be used as an approximation. For liquid water, the form factor to be used is $F_{w,liq}$.

In the present calculations, the form factor $F_{w,liq}$ has been used, together with the total Rayleigh cross-section, obtained by numerical integration of the Thomson formula weighted by $F^2_{w,liq}$.

4. Results

4.1. Pencil beam

Let dS be a surface element located on the reception sphere and including point A (figure 1). Let dE be the single scattered energy which is most probably received by dS when an incident photon of energy E_0 arrives. dE/dS is the single-scattered energy which is received per unit surface area at point A(φ) of the reception sphere.

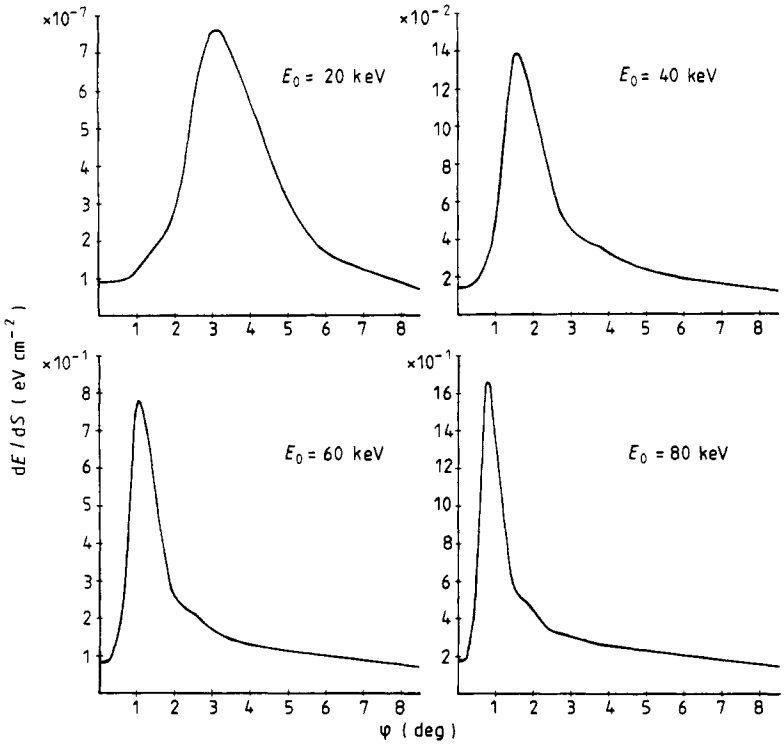

Figure 4. Pencil beam geometry. Single-scattered energy dE/dS plotted against φ for various values of E_0, the energy of the incident photons.

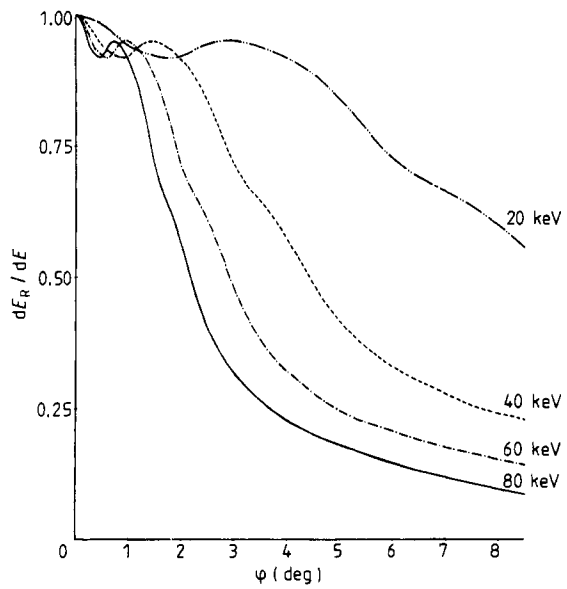

Figure 5. Pencil beam geometry: proportion of Rayleigh scattering. (dE_R/dE) plotted against φ, where dE is the single-scattered energy received by dS and dE_R the single-scattered energy received by dS, due to Rayleigh scattering.

Figure 4 shows dE/dS plotted against φ for incident photon energies of 20, 40, 60 and 80 keV. The shape of the curves for small values of φ is due to the use of the form factor $F_{w,liq}$.

Figure 5 shows the contribution of the Rayleigh scattering to single scattered energy.

4.2. Conical beam

Figure 6 shows the ratio of single-scattered to transmitted energies plotted against φ for incident photon energies of 20, 40, 60 and 80 keV. As the transmitted energy does not depend upon φ, figure 6 also gives the shape of the single-scattered energy versus φ. Table 1 gives the ratio of single-scattered to transmitted energies, averaged over the cone.

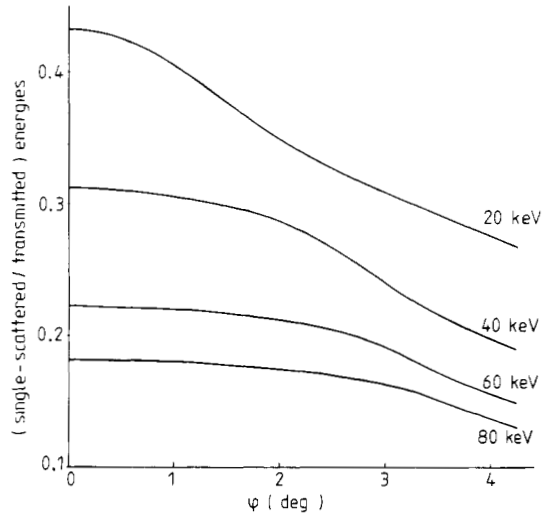

Figure 6. Conical beam goemetry: ratio of single-scattered to transmitted energies plotted against φ.

When the incident photon energy is only 20 keV, the scattered and transmitted energies (table 1) reaching the reception sphere are extremely small due to attenuation in the phantom. These photons will therefore not contribute measurably to the image-forming process with a phantom of this thickness.

Table 1. Conical beam: ratios averaged over the cone.

	Ratios		
Energy (keV)	Single-scattered / Transmitted	Rayleigh / Compton + Rayleigh	Transmitted / Incident
20	0.32	0.91	0.43 *E*-7
40	0.25	0.75	0.0034
60	0.19	0.60	0.012
80	0.16	0.49	0.020

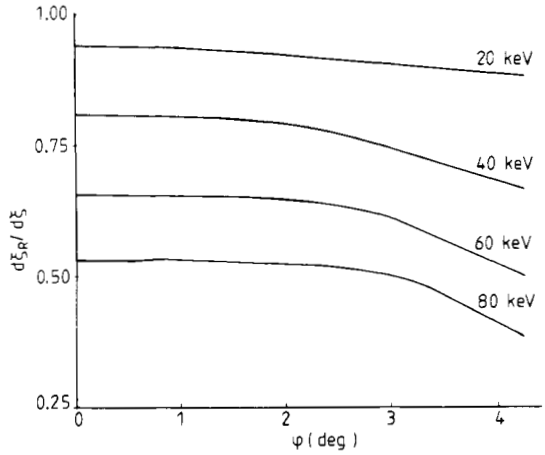

Figure 7. Conical beam geometry: proportion of Rayleigh scattering ($d\xi_R/d\xi$) plotted against φ. $d\xi$ is the single-scattered energy received by dS, and $d\xi_R$ the single-scattered energy received by dS, due to Rayleigh scattering.

Figure 7 shows the contribution of Rayleigh scattering to single scattered energy, as a function of φ. After averaging over the cone, this contribution is found to be equal to 91% at 20 keV and 49% at 80 keV (table 1).

5. Discussion

Several points must be stressed:

(i) Only single-scattered energy has been calculated.

(ii) The incident radiation has been assumed to be monoenergetic.

(iii) The effect of grids and antiscatter devices has not been taken into account.

(iv) The problems related to detector efficiency have not been taken into account.

Such problems have been studied in detail by Kalender (1981). In the single-scattered energy received by a surface element, we have counted the energies of all photons arriving on such an element, whatever their energies and directions may be.

5.1. Dependence on incident energy

Most of the previous studies defined the 'scatter fraction' as the ratio of scattered to (scattered + transmitted) energies. A major concern of these studies has been to determine the dependence of the scatter fraction on incident energy (Dick *et al* 1978, Kalender 1981). As we have only calculated single-scattering, we have been unable to express our results in terms of scatter fraction and we have used the ratio of single-scattered to transmitted energies. We have found a strong dependence of this ratio upon incident energy (figure 6 and table 1).

5.2. Polarisation

The incident beam has been assumed to be unpolarised. This is consistent with the differential cross-sections used in this paper (section 3). It must be noticed, however, that such cross-sections are no longer valid when multiple scattering is taken into account, for, even when the incident beam is unpolarised, the Rayleigh scattered beam is partially polarised (Kissel 1981, private communication).

5.3. Case of body tissues

The present calculations only concern a water phantom. It is likely that body tissues do not have the same scattering properties as liquid water. Scattering cross-sections of body tissues can be estimated using appropriate sum rules, but it has been seen in section 3.3 that the sum rule for Rayleigh scattering was not accurate, especially at small angles. The $F_{w,liq}$ data, used in this paper, have been derived from the results of Narten and Levy (1971), whose aim was to study the structure of liquid water. It is likely that similar data on body tissues could be obtained in the same way, using methods or results of solid state physics.

6. Conclusion

In a geometrical arrangement which approaches that of the dynamic spatial reconstructor (DSR), the ratio of single-scattered to transmitted energies is strongly dependent upon the incident energy: in the range 20 to 80 keV it varies from 0.32 to 0.16. The contribution of the Rayleigh effect to single scattering is of the order of 90% at 20 keV and 50% at 80 keV.

Acknowledgments

The calculations were performed at the Ecole Nationale des Ponts et Chaussées. We wish to thank the staff of the computing centre and especially Mr Nouvel, Mr Philipp and Mr Pingeon.

Résumé

Calcul de la diffusion primaire des rayons X en radiodiagnostic.

L'énergie diffusée simple a été calculée dans le cas de l'eau, dans une disposition géométrique qui se rapproche de celle du reconstructeur dynamique DSR. On a utilisé des données récentes sur les sections efficaces différentielles de diffusion Rayleigh par l'eau liquide. On trouve que le rapport (énergie diffusée simple)/(énergie transmise) dépend de l'énergie du photon incident: entre 20 keV et 80 keV, ce rapport varies de 0,32 à 0,16. La contribution de l'effet Rayleigh à l'énergie diffusée simple est de l'ordre de 90% à 20 keV et de l'ordre de 50% à 80 keV.

Zusammenfassung

Berechnung der Einfachstreuung von Röntgenstrahlen in der Röntgendiagnostik.

Die Energie nach Einfachstreuung wurde berechnet für ein Wasserphantom in einer speziellen geometrischen Anordnung. Dabei wurden neue Werte der differentiellen Rayleigh-Wirkungsquerschnitte für Wasser benutzt. Das Verhältnis für Einfachstreuung ist abhängig von der einfallenden Energie: es variiert im Bereich 20–80 keV zwischen 0.32 und 0.16. Der Beitrag der Rayleigh-Streuung zur Einfachstreuung beträgt etwa 90% bei 20 keV und 50% bei 80 keV.

References

Blum L 1971 *J. Comput. Phys.* **7** 592–602
Burgess A E and Pate G 1981 *Med. Phys.* **8** 33–8
Cacak R K 1981 *Med. Phys.* **8** 249
Dick C E, Soares C G and Motz J W 1978 *Phys. Med. Biol.* **23** 1076–85
Guinier A 1964 *Théorie et Technique de la Radio-Cristallographie* (Paris: Dunod) pp 426–8

Hubbell J H, Veigele W J, Briggs E A, Brown R T, Cromer D T and Howerton R J 1975 *J. Phys. Chem. Ref. Data* **4** 471–538, erratum in 1975, *J. Phys. Chem. Ref. Data* **6** 615–6
Hubbell J H and Overbo I 1979 *J. Phys. Chem. Ref. Data* **8** 69–105
James R W 1962 *The Optical Principles of the Diffraction of X-rays* (London: Bell) pp 29–458
Joseph P M and Spital R D 1981 *Med. Phys.* **8** 551
Kalender W 1981 *Phys. Med. Biol.* **26** 835–49
Kinsey J H and Orvis A L 1981 *IEEE Trans. Nucl. Sci.* **NS-28** 1732–5
Levine M M and Hale J 1980 *Phys. Med. Biol.* **25** 545–8
Moon P B 1950 *Proc. Phys. Soc.* A**63** 1189–96
Moore R, Korbuly D and Amplatz K 1976 *Radiology* **120** 713–7
Morin L R M 1982 *J. Phys. Chem. Ref. Data* **11** 1091–8
Narten A H and Levy H A 1971 *J. Chem. Phys.* **55** 2263–9
Reiss K H and Steinle B 1973 *Phys. Med. Biol.* **18** 746–7
Rudin S and Bednarek D R 1980 *Proc. SPIE* **233** 38–42
Schultz E and Felix R 1980 *Med. Prog. Technol.* **7** 169–81
Scofield J H 1973 *Theoretical Photo-ionisation Cross-sections from* 1 *to* 1500 keV UCRL-51326
Stargardt A and Angerstein W 1975 *Fortschr. Geb. Röntgenstrahl.* **123** 364–9
Stonestrom J P and Macovski A 1976 *IEEE Trans. Nucl. Sci.* **NS-23** 1453–8